P3.8 DETECTING VOLCANIC ASH AND BLOWING DUST USING GOES, MODIS, AND AIRS IMAGERY

Bernadette H. Connell
Cooperative Institute for Research in the Atmosphere (CIRA)
Colorado State University, Fort Collins, Colorado

Fred J. Prata
CSIRO Atmospheric Research
Aspendale, Victoria
Australia

1. INTRODUCTION

With the various satellite techniques that exist to identify volcanic ash and aerosol and dust, there is no one technique that will work everywhere, every time. Imagery from the geostationary operational environmental satellite (GOES) has been particularly useful in tracking volcanic plumes and dust and their evolution over time. The moderate resolution imaging spectroradiometer (MODIS) is a newer polar orbiting satellite instrument that offers higher spatial resolution and increased spectral resolution over the GOES sensor (the VISSR) but at a lower temporal frequency. The Atmospheric Infrared Sounder (AIRS) sensor offers hyperspectral resolution at a reduced spatial and temporal resolution. The combination of these three instruments will help provide a better picture of what is being observed for volcanic ash and dust features and how to better utilize the data in the future.

The brightness temperature difference between the 11.0 and 12.0 µm imagery has been used with much success over the last 15 years to identify volcanic ash plumes and blowing dust. In terms of volcanic ash, the main drawback to this technique tends to occur in very humid environments, when the ash is low in concentration or when the ash/dust is mixed with meteorological cloud. Other image products using the short wave infrared imagery around 3.9 µm and the longer waver imagery at 8.5 µm have experienced limited success in identifying the ash and dust plumes. One example each of dust and volcanic ash for day time conditions will be presented here showing the various products available from the GOES, MODIS, and AIRS instruments. The signature of the products for ash, dust, and cloud features, mainly in the form of brightness temperature differences or a measure of difference in reflectance, will be compared with corresponding spectral curves available from AIRS imagery. A couple of points will be highlighted: "thin" plumes versus optically "thick" plumes, and ash alone or ash and aerosol versus dust.

Corresponding author address: Bernadette Connell, CIRA at Colorado State University, 1375 Campus Delivery, Fort Collins, CO 80523-1375; e-mail: connell@cira.colostate.edu

2. TECHNIQUES

Prata (1989a, 1989b) used the brightness temperature (BT) difference between the bands centered near 11.0 and 12.0 µm to detect ash while Shenk and Curran (1974) used this difference to detect dust storms. The BT11.0 – BT12.0 is generally negative for ash and dust and positive for ice and water clouds. Theoretically, if the ash cloud is optically thin, with an optical thickness less than 3, the particle size and optical thickness can be calculated assuming some constituent material. If the cloud is optically "thick", the satellite signature of the ash cloud should resemble that of the constituent material. It is possible to have an optically thick and an optically thinner cloud have the same brightness temperature difference. Is it possible to tell the difference between the two clouds?

The use of the 3.9 µm channel for detection of ash has been demonstrated by Ellrod et al. (2003) and has been shown by Ackerman (1989) for the detection of dust. The 3.9 µm channel senses solar radiation as well as emitted radiation; hence the imagery is interpreted differently during the day than at night. For the daytime scenes, scattering of shortwave radiation by particles enhances the reflectance. For water particles, the reflectance is inversely proportional to the drop size. Small water droplets are strongly reflective, larger ice particles are less reflective. Volcanic ash and dust samples show higher reflectance in the 3.9 µm region than in the 10.7 or 12.0 µm regions (Schneider and Rose, 1994; Salisbury and Walter, 1989). Dust and ash cannot generally be distinguished uniquely using the 3.9 µm and 10.7 µm or 12.0 µm combinations, but will appear more like water or very thin ice cloud that is composed of very small particles (less than 5 µm).

The region around 8.0 – 9.5 µm is sensitive to dust, ash, and sulfate aerosols. Baran et al. (1993) and

Ackerman and Strabala (1994) looked into the use of the 8.3 µm channel on the high resolution infrared sounder (HIRS) system for the detection of H_2SO_4 aerosol from the Pinatubo eruption. Over oceans there is a small negative BT8.3 – BT12.0 background signature due to moisture. The BT8.3 – BT12.0 becomes more negative for H_2SO_4 aerosol, and also becomes more negative for an increase in atmospheric water vapor. The BT8.3-12.0 is positive for ice.

For dust, Ackerman (1997) found that a high optical depth results in positive BT8-BT11. Wald et al. (1998) simulated the MODIS capabilities of the detection of mineral dust over desert using the 8.0 - 12.0 µm region. Using various particle sizes of quartz and varying the optical depth, they found that the BT12.0 – BT 8.0 was the smallest (ie. negative) (positive for BT8.0 – BT12.0) for 2 µm particles and small optical depth and was positive for large optical depth, taking on the signature of the quartz sand background.

Based on these few results, the signal observed in the BT8.0 – BT12.0 products could be challenging to interpret in a volcanic cloud that is composed of ash and aerosol. Depending on the size of the particles and the concentration, the ash could either negate the signal of the sulfate aerosol or make it stronger.

Dust is similar to volcanic ash in many ways. Examining case studies of dust along with ash can help to further delineate their similarities and differences and aid in better detection techniques.

3. Examples

3.1 *Dust*

An example of blowing dust during the day is shown in figure 1 for 18 April 2004 at 19:30 UTC. The extent of the plume is highlighted with dashed lines in the MODIS BT11.0-BT12.0 (figure 1c) image. Both the MODIS and the GOES difference product for BT11-BT12 (figure 1c and 1a respectively) show similar values (most negative value = -2.5K, average = -2.0K and -1.5K respectively) for the thicker part of the plume, represented by the circle labeled y. They also show similar values (1.0K and 0.0K = the most positive values respectively, average=-0.5K) for the thinner portion of the plume labeled as circle x. The extent of the dust plume for these difference products agrees with that shown by the GOES reflectance product in figure 1b. In this product, the dust as well as low level water clouds appear more reflective. In contrast, the MODIS BT8.5-BT12.0 product shown in figure 1d represents the plume with values -1.0K – 0.0K in what appears to be the densest region labeled as circle y. In the circled region labeled as x, the most negative value is -7.0K with an average value of -5.0K. Points in this region are expected to take on the ground signature in this area.

Figure 2a and 2b. shows the AIRS spectral plot of temperature versus wavelength for the shortwave (3.7 – 4.1 µm) and longwave region (8.0 – 13.0 µm) for a point within the y circle on figure 1 (open circle) . A clear background point to the east of this point is also presented for comparison (open triangle). A slightly positive slope can be noted in the 10.0 – 12.0 µm region, accounting for the small negative BT 11.0 – 12.0 difference. Points that are cooler than the main portion of the spectrum in the 10.0 – 12.0 µm region are circled (region u) and indicate low level moisture and hence that the plume is "thin". Notice that the dust spectral values in the shortwave region are warmer than the background values indicating increased reflectance for the dust. To illustrate a "thick" plume, a spectral plot from a dust plume in Iraq on 25 June 2003at 10:36 UTC is presented in figure 2c and 2d. Except for the dip around 11.5 µm there are essentially no points in the 10.0 – 12.0 µm region (circled region v) that are cooler than the main portion of the spectrum indicating that the plume is relatively thick and moisture below it cannot be sensed. In the shortwave region, temperatures for the dust are much warmer than in the longwave region as compared to the background temperature differences and indicate increased reflectance.

3.2 *Volcanic Ash*

An example of volcanic ash detection during the day is shown in figure 3 for 6 April 2005 at 03:25 UTC for GOES-9 (03:35 for MODIS) for the eruption of Anatahan in the Marianna Islands. The extent of the plume is outlined. There are 3 distinct portions: one that potentially contains ice and SO_2 (region R), another that is primarily thick ash (region M), and another that is low in ash concentration (region L). Both the MODIS and the GOES difference product for BT11-BT12 (figure 3c and 3a respectively) show similar pattern and values. There are negative values of approximately -1.5K in region L which represents thin ash, values of -3.0K to -5.0K in region M, which represents thicker ash, and values of +5.0K to +7.0K in region R, which represents ice and potentially SO_2.

The reflectivity product in figure 3b shows more reflective cloud for region M and less reflective cloud in the other 2 regions. Ice in general would appear much less reflective than is represented in figure 3b. The somewhat reflective appearance of region R could be due to smaller particles (<5 µm).

In contrast, the MODIS BT8.5-BT12.0 product shown in figure 3d has a mix of positive and negative BT differences. The largest positive values (+10.0K) are in region R with the other regions having values as large as +6.0K. The negative values approach -3.5 to -5.5K in all regions. The wide difference in values could be due to different particle sizes and concentrations as well as a mix of ash and sulfate aerosols.

Figure 4. shows the AIRS Aqua spectral plot of temperature versus wavelength for the shortwave (3.7 – 4.1 µm) and longwave region (8.0 – 13.5 µm) for one point each in region L and region M in figure 3. A positive slope is noted for both points. Notice that there are cooler points than the main spectral curve between 10.0 to 12.0 µm for region L (circled region s), but not for region M (circled region t). This indicates a thinner and a thicker ash plume respectively, similar to the dust cases. The spectrum is not sampled between 8.2 and 8.8 µm. Here we see quite a jump in temperatures for

both the thin and the thicker plumes. This is not seen in the dust example. Perhaps this is due to the presence of sulfate aerosols and/or a difference in particle size, concentration, and constituent. There is quite a bit of scatter in the points between 3.7 and 3.8 μm for the thin ash (circled region q) as compared to very little scatter for the thick ash (circled region r). There is also a larger temperature difference between the shortwave and longwave values for region M than for region L. Both the less scatter of points in the shortwave region and the increased temperature difference between the longwave and shortwave indicate a thick ash plume with greater reflectance at the shorter wavelengths.

4. CONCLUDING REMARKS

Examples of satellite techniques using GOES and MODIS imagery were presented to show what is often "detected" for volcanic ash and dust. The AIRS data add an interesting dimension to the interpretation techniques used to infer the presence of volcanic ash and dust. Two examples were presented here which highlight features that could be used to identify thick versus thin plumes. More examples will be explored in the future to determine if the features are robust or to determine if there are other factors that are affecting what is observed.

5. ACKNOWLEDGMENTS

Funding for this study is made available through NOAA Grant NA67RJ0152.

The MODIS and AIRS data used in this study were acquired as part of the NASA's Earth Science Enterprise and archived and distributed by the Goddard Earth Sciences (GES) Data and Information Services Center (DISC) Distributed Active Archive Center (DAAC). We are very grateful to have access to this data.

6. REFERENCES

Ackerman, S. A., 1989: Using the radiative temperature difference at 3.7 and 11 μm to track dust outbreaks. *Remote Sens. Environ*. **27**:129-133.

Ackerman, S. A., 1997: Remote sensing aerosols using satellite infrared observations. *J. Geophys. Res.,* **102** (D14): 17,069-17,079.

Ackerman, S. A., and K. I. Strabala, 1994: Satellite remote sensing of H2SO4 using the 8- to 12- μm window region: Application to Mount Pinatubo. *J. Geophys. Res.*, **99** (D9): 18,639-18,649.

Baran, A. J., J. S. Foot, and P. C. Dibben, 1993: Satellite detection of volcanic sulphuric acid aerosol. *Geophys. Res. Lett.,* **20** (17):1799-1801.

Ellrod, G. P., B. H. Connell, D. W. Hillger, 2003: Improved detection of airborne volcanic ash using multi-spectral infrared satellite data. *J. Geophys. Res.*, **108** (D12): Art. No. 4356 Jun 21.

Prata, A. J., 1989a: Observations of volcanic ash clouds in the 10-12 μm window using AVHRR/2 data. *Int J. Remote Sensing*, **10**(4-5):751-761.

Prata, A. J., 1989b: Infrared radiative transfer calculations for volcanic ash clouds. *Geophsy. Res. Lett.,* **16**(11): 1293-1296.

Salisbury, J. W., and L. S. Walter, 1989: Thermal infrared (2.5-13.5 um) spectroscopic remote sensing of igneous rock types on particulate planetary surfaces. *J. Geophys. Res*., **94**, No. B7, 9192-9202.

Schneider, D. J., and Rose, W. I., 1994: Observations of the 1989-1990 Redoubt volcano eruption clouds using AVHRR satellite imagery. In: Volcanic ash and aviation safety: Proceedings of the First International Symposium on Volcanic Ash and Aviation Safety. U. S. Geological Survey Bulletin 2047, 405-418.

Shenk, W. E., and R. J. Curran, 1974: The detection of dust storms over land and water with satellite visible and infrared measurements. *Mon. Weather Rev.*, **102**: 830-837.

Wald, A. E., Y. J. Kaufman, D. Tanré, and B. –C. Gao, 1998: Daytime and nighttime detection of mineral dust over desert using infrared spectral contrast. *J. Geophys. Res.,* **103** (D24): 32,307-32,313.

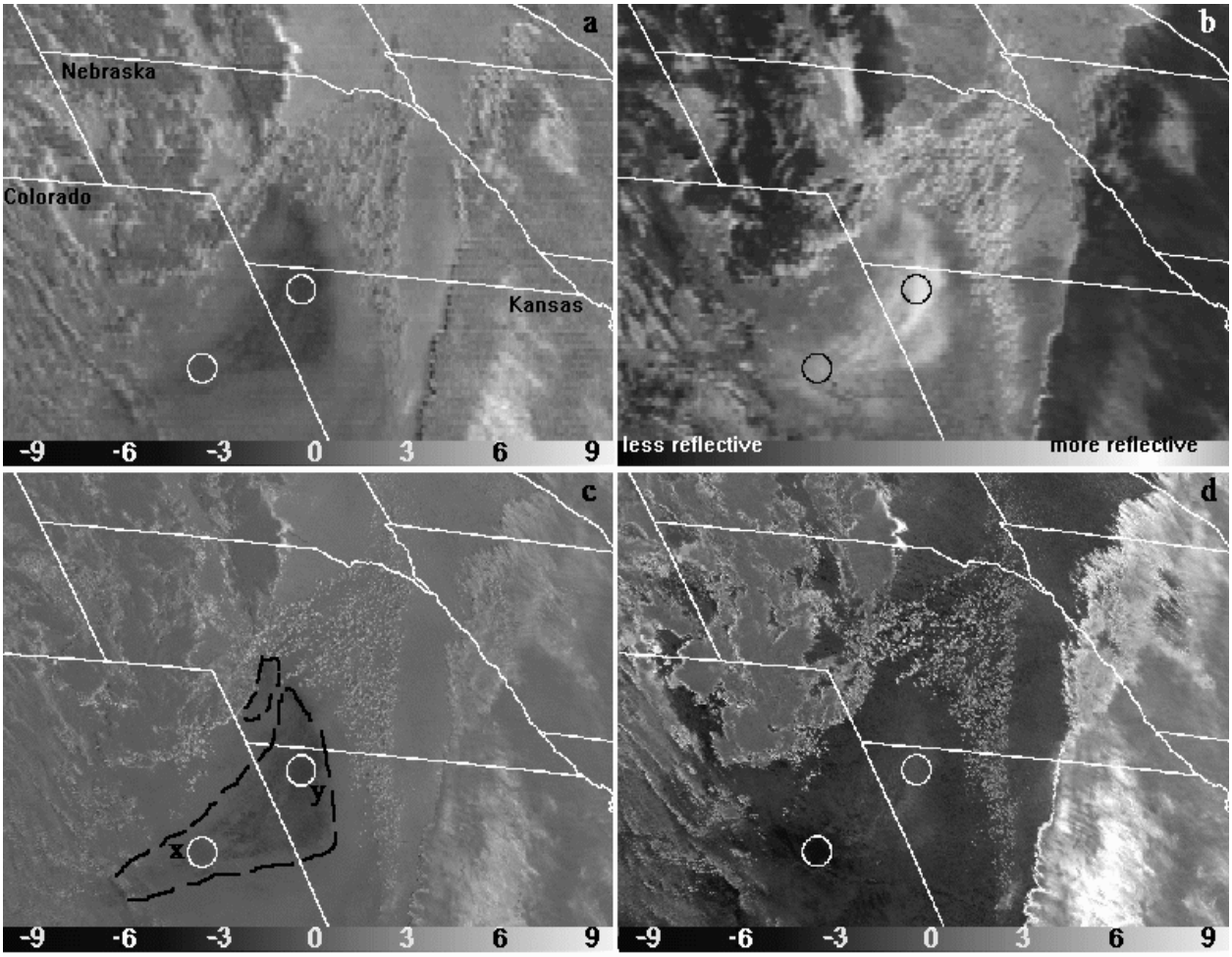

Figure 1. Satellite imagery products showing the dust plume extending from Colorado into Kansas and Nebraska on 18 April 2004, GOES and MODIS Aqua at 19:30 UTC. a) GOES BT10.7-BT12.0, b) GOES reflectivity product using the 3.9 and 10.7 µm channels c) MODIS BT11.0-BT12.0, the dashed line indicates the plume outline, and d) MODIS BT8.5-BT12.0.

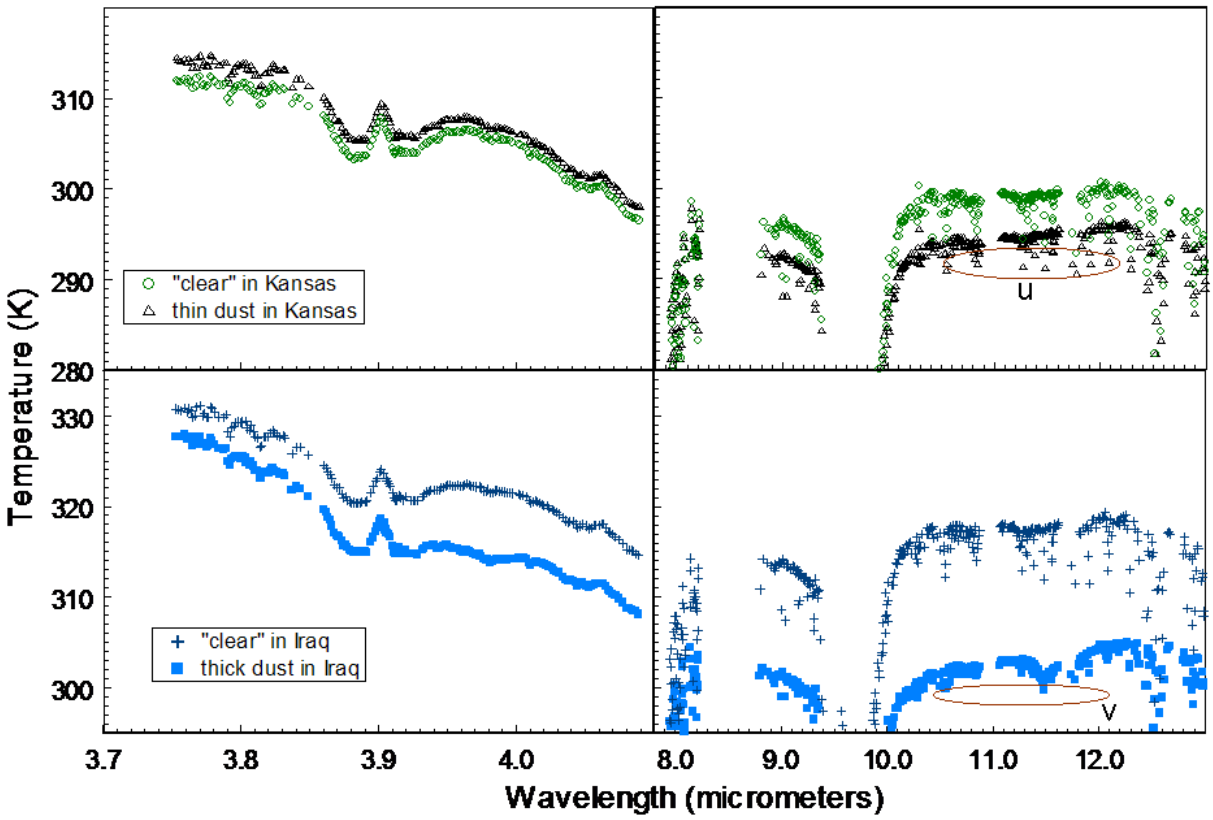

Figure 2. Top two graphs: AIRS Aqua spectral plot of temperature versus wavelength for the shortwave (3.7 – 4.1 μm) and longwave region (8.0 – 13.0 μm) for a point within the y circle representing thin dust (open circle), and a point to the east of this representing clear ground (open triangle) on Figure 1. Data are for 18 April 2004 at 19:30 UTC Bottom two graphs: comparison examples of thick dust (closed square) and clear ground (plus) in Iraq on 25 June 2003at 19:30 UTC. Circled regions u and v are described in text.

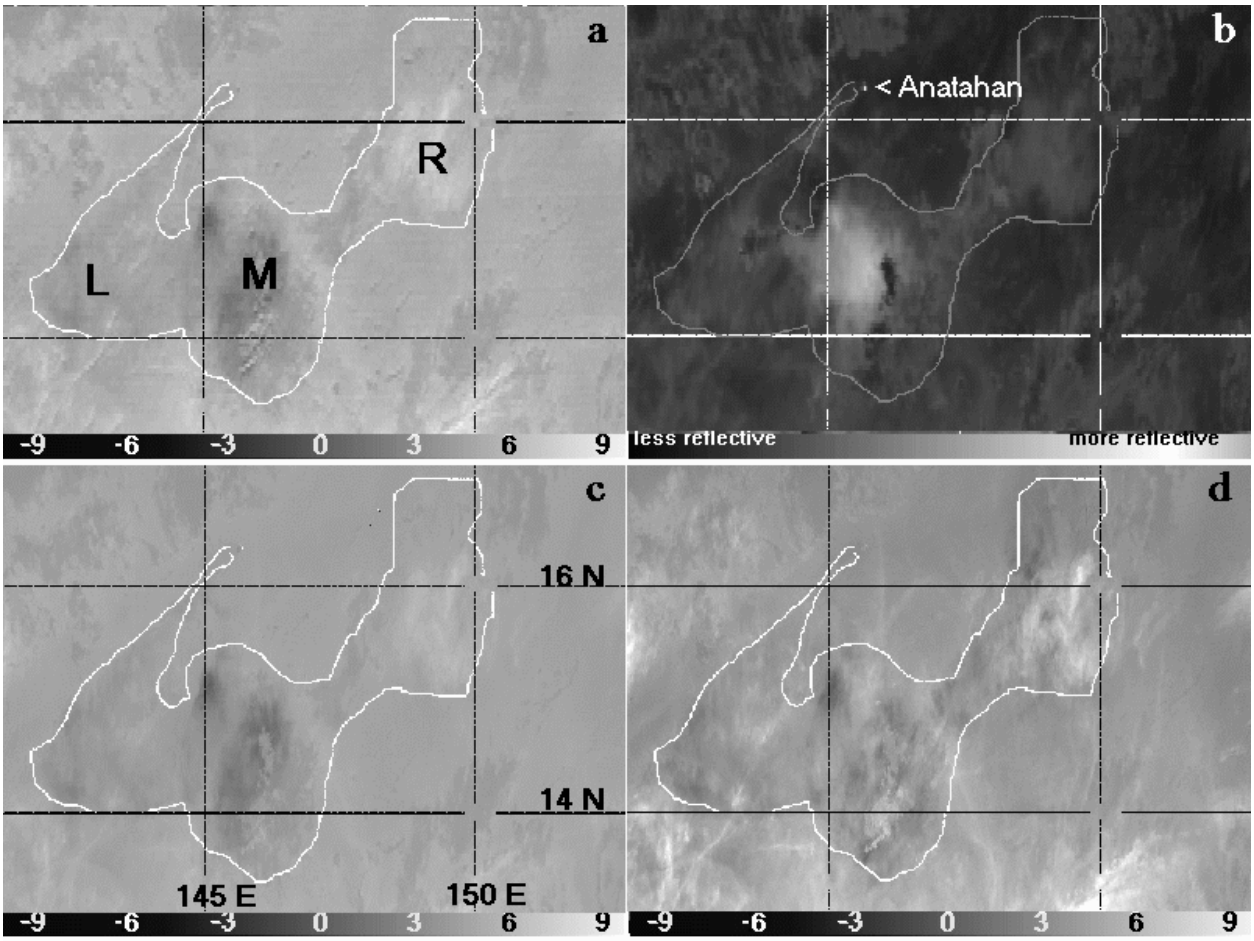

Figure 3. Satellite imagery products showing the volcanic ash and aerosol plume extending from Volcano Anatahan on 6 April 2005, GOES-9 and MODIS Aqua at 03:25 and 03:35 UTC respectively. a) GOES BT10.7-BT12.0, b) GOES reflectivity product using the 3.9 and 10.7 µm channels c) MODIS BT11.0-BT12.0, and d) MODIS BT8.5-BT12.0. The extent of the plume is outlined in white.

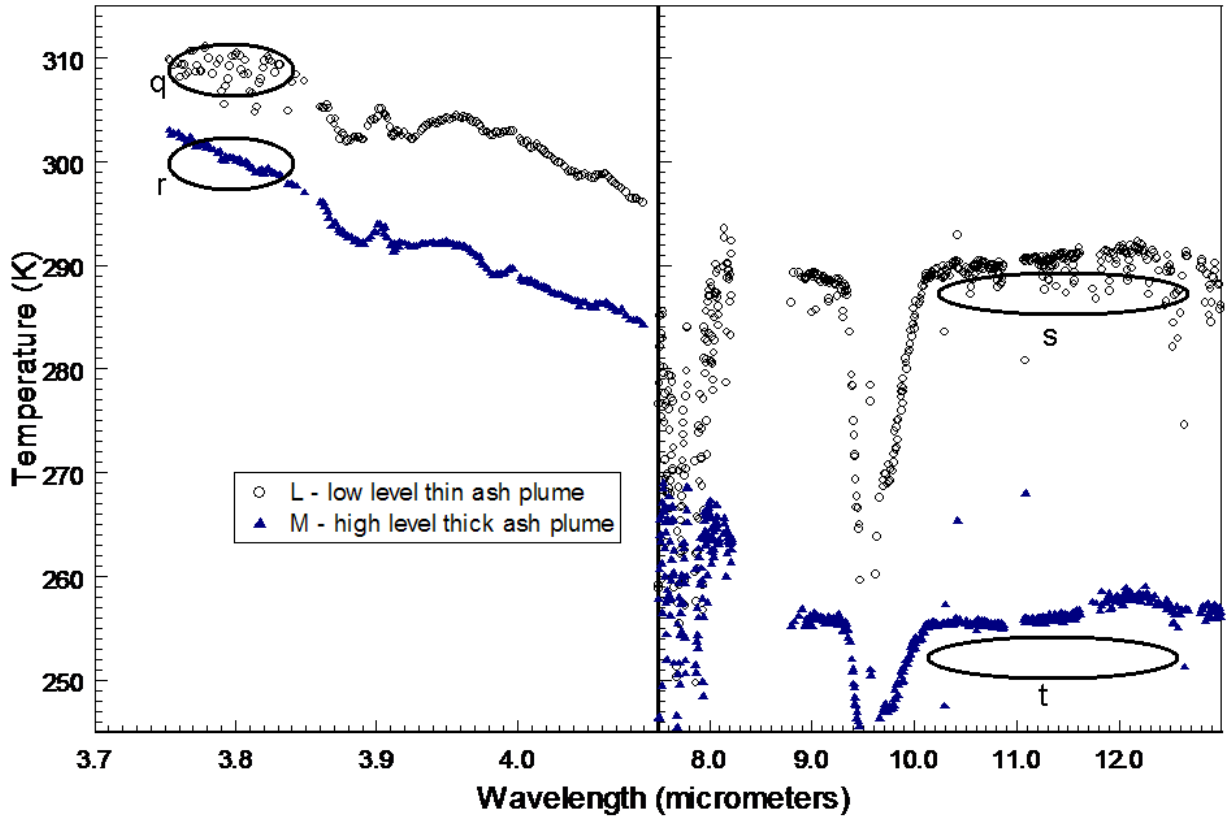

Figure 4. AIRS Aqua spectral plot of temperature versus wavelength for the shortwave (3.7 – 4.1 μm) and longwave region (8.0 – 13.5 μm) for one point each in region L (open circle) and region M (closed triangle) in Figure 3. Data are for 6 April 2005 at 03:36 UTC for the Anatahan eruption. Circled regions q, r, s, and t are explained in the text.